Int J Thermophys (2017) 38:184
DOI 10.1007/s10765-017-2321-8

TEMPMEKO 2016

Co–C and Pd–C Eutectic Fixed Points for Radiation Thermometry and Thermocouple Thermometry

L. Wang[1]

Received: 19 July 2016 / Accepted: 23 October 2017 / Published online: 1 November 2017

Abstract Two Co–C and Pd–C eutectic fixed point cells for both radiation thermometry and thermocouple thermometry were constructed at NMC. This paper describes details of the cell design, materials used, and fabrication of the cells. The melting curves of the Co–C and Pd–C cells were measured with a reference radiation thermometer realized in both a single-zone furnace and a three-zone furnace in order to investigate furnace effect. The transition temperatures in terms of ITS-90 were determined to be 1324.18 °C and 1491.61 °C with the corresponding combined standard uncertainty of 0.44 °C and 0.31 °C for Co–C and Pd–C, respectively, taking into account of the differences of two different types of furnaces used. The determined ITS-90 temperatures are also compared with that of INRIM cells obtained using the same reference radiation thermometer and the same furnaces with the same settings during a previous bilateral comparison exercise (Battuello et al. in Int J Thermophys 35:535–546, 2014). The agreements are within $k = 1$ uncertainty for Co–C cell and $k = 2$ uncertainty for Pd–C cell. Shapes of the plateaus of NMC cells and INRIM cells are compared too and furnace effects are analyzed as well. The melting curves of the Co–C and Pd–C cells realized in the single-zone furnace are also measured by a Pt/Pd thermocouple, and the preliminary results are presented as well.

Keywords Eutectic fixed point · Point of inflection (POI) · Radiation thermometry · Thermocouple thermometry · Transition temperature

Selected Papers of the 13th International Symposium on Temperature, Humidity, Moisture and Thermal Measurements in Industry and Science.

✉ L. Wang
wang_li@nmc.a-star.edu.sg

[1] National Metrology Centre (NMC), Agency for Science, Technology and Research (A*STAR), Singapore, Singapore

1 Introduction

As is well known, a set of high-temperature fixed points (HTFPs) made of metal–carbon eutectics with an interpolation equation provides an alternative to the realization of ITS-90 above 962 °C [1–5]. The HTFPs method, besides reducing extrapolation errors at higher temperatures existing in the current defined ITS-90 realization method, offers other advantages such as avoiding complex and time-consuming measurements of spectral responsivity of the reference radiation thermometer used for the ITS-90 realization. The HTFPs are also useful for high-temperature thermocouple calibrations which are traditionally done at the melting points of copper (1084.62 °C) and palladium (1552 °C) [6–9]. Between the copper and the palladium points, the temperature scale is realized using the thermocouple interpolation equation. As there is a big gap between the two temperature points, the interpolation error remains a major concern. The Co–C (1324 °C) and Pd–C (1492 °C) eutectic fixed points having transition temperatures between these two temperatures fill this gap well and are now adopted by many national metrology institutes. For these purposes, NMC established Co–C and Pd–C eutectic fixed points as temperature standards for both radiation thermometry and thermocouple applications.

2 Description of Cells

2.1 Design of Cells

Crucibles used for both radiation thermometry and thermocouple thermometry have been designed previously by several authors [10–12]. However, some of these designs require either a special furnace or a complex filling mechanism. A simple design is utilized, which includes a thermometer well long enough to accommodate a thermocouple and an aperture for a radiation thermometer use. As shown in Fig. 1, the thermo-well is 8 mm in diameter and 116 mm long which is deemed enough for thermocouple immersion. A removable aperture of 3 mm can be inserted into the thermo-well for radiation thermometer measurement. Two layers of C/C sheets are inserted in between the cell body and the graphite sleeve both on the bottom and on the side. For the Pd–C cell, the side of the thermo-well in contact with the eutectic material is covered by an additional graphite sheath and a layer of graphite sheet inserted in between the thermo-well and the graphite sheath, in order to protect the thermocouples from Pd penetration through the wall of the thermo-well. This arrangement is very similar to the design of Ogura et al. [7]. The effective inner volume is around 28 cm^3 for the Co–C cell and 20 cm^3 for the Pd–C cell. Sources of materials and their impurities/purities used for different parts and eutectics are given in Table 1.

2.2 Filling Process

Firstly, the metal in either shot or powder form was mixed with graphite powder according to the eutectic composition. The mixture was then placed in the pre-assembled cell without the thermo-well. The mixture was melted and solidified in an argon envi-

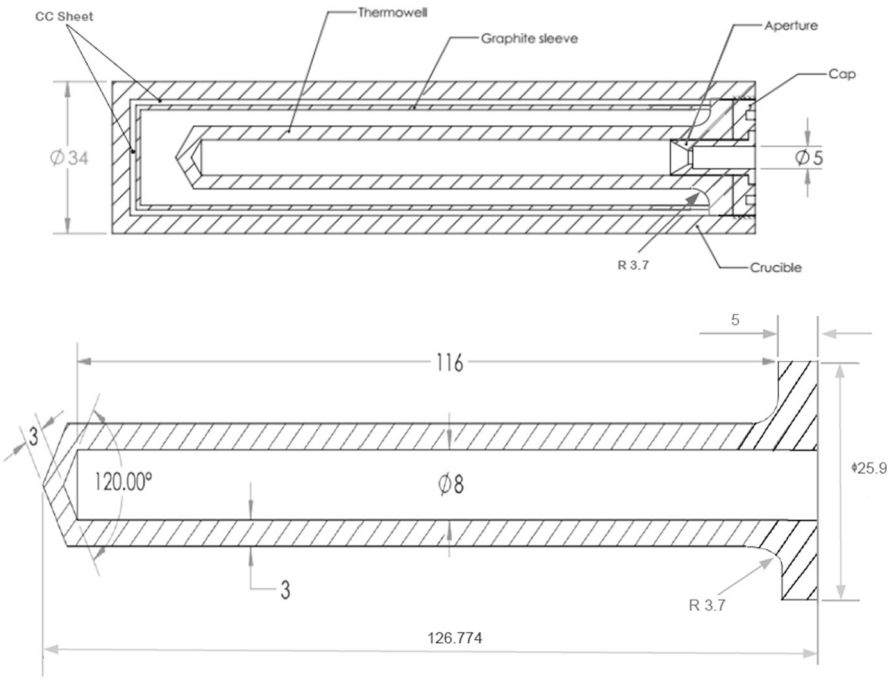

Fig. 1 Diagram of cell and cavity design

Table 1 Information on materials used

Item	Source	Impurity/purity
Graphite parts except Pd–C thermo-well sheath	Mersen (known as Carbone Lorrane until 2010)	Ash content $< 0.002\,\%$
Pd–C thermo-well sheath	POCO graphite Inc.	< 5 ppm
C/C sheet/Graphite sheet	Toyo Tanso Co., Ltd.	< 10 ppm
Graphite powder	Alfa14734.TA	99.9999 %
Co shot	JX Nippon Mining & Metals	99.999 %
Pd powder	Ishifuku Metal Industry Co. Ltd.	99.997 %

ronment in a graphite furnace placed vertically (details of the furnace are described in Sect. 3). A heating/cooling rate of about 10 °C · min was applied in the temperature range about ±30 °C of the eutectic temperature. The same process was repeated if the mixture could not be accommodated the first time. When all the mixture had solidified into the cell, the thermo-well was inserted into the cell guided by a funnel and the melting process was repeated again. Two graphite weights were placed on top of the funnel to help the thermo-well sink during the melt. After the thermo-well was properly inserted into the cell, the solidification process started. After cooling down, the cell was taken out, sealed, and ready for use.

3 Furnaces and Reference Radiation Thermometer

To measure the eutectic temperatures of Co–C and Pd–C, a graphite furnace capable of heating up to 2000 °C [13], named as single-zone furnace, was used. A special designed cell holder used to contain the eutectic cell was installed into the furnace cavity as shown in Fig. 2. The eutectic cell was placed at the bottom of the cell holder where the temperature distribution was more uniform, as measured by a type B thermocouple at 1500 °C previously. The furnace was placed vertically for filling the cells and measuring with thermocouples and placed horizontally for measuring with the radiation thermometer. In order to evaluate the furnace effect on the eutectic temperatures, a horizontal three-zone furnace capable of operating up to 1800 °C was used for the same measurements. In this arrangement, the cell was placed in a ceramic tube with graphite protective blocks and cones behind and in front as shown in Fig. 3. The whole assembly was then placed in the working tube of the furnace. It was discovered in a previous study [14] that the furnace temperature was uniform within ± 0.2 °C up to 1500 °C in a zone about ± 50 mm from the center of the furnace. Therefore, the cell was located in the uniformed zone accordingly.

The transition temperatures of the eutectic cells were measured by NMC's reference radiation thermometer. The details of the thermometer are described in [13]. It

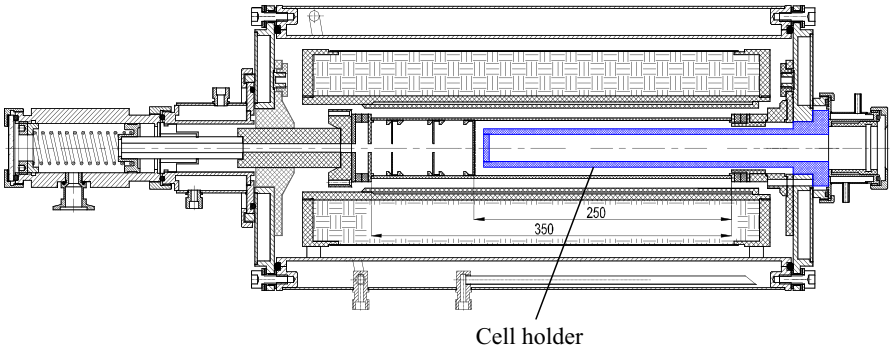

Fig. 2 Diagram of graphite furnace with cell holder

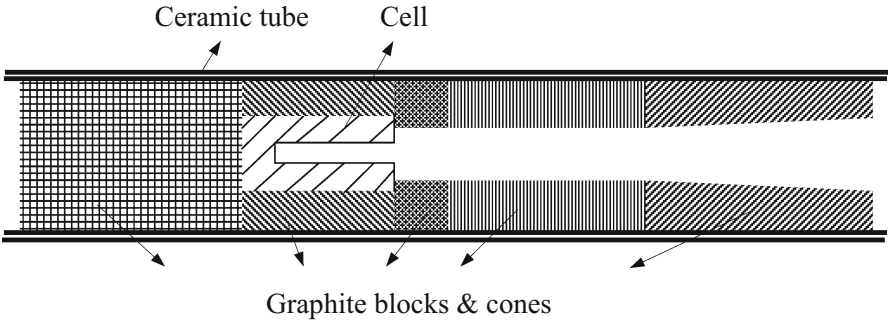

Fig. 3 Schematic drawing of assembly of ceramic tube, cell, and protective blocks and cones in the three-zone furnace

is calibrated according to the ITS-90 definition, following NMC procedures for realization of ITS-90 above silver point. All measurements were performed at a working wavelength of 650 nm.

4 Measuring with the Reference Radiation Thermometer and Results

4.1 Measurements

In the case of the single-zone furnace, ± 10 K, − 5 K to + 10 K, and − 5 K to + 15 K furnace temperature offsets were used to induce the Co–C phase transitions. In the case of the three-zone furnace, an offset of −5 K to + 10 K was used instead. Similarly, the Pd–C phase transitions were realized with melts and freezes induced by ± 10 K, −5 K to + 10 K, and −5 K to + 15 K offsets in both furnaces. These temperature settings induced better plateaus as evidenced by the previous study [13]. The heating rate was about 10 °C·min for the single-zone furnace and about half the speed for the three-zone furnace due to its higher thermal inertia and the characteristics of the furnace.

The first analysis of the melting curves was to study the point of inflections (POIs). We used three different methods to carry out this study. The first method was named as the average method. It used the standard deviations of the running averages to determine the entry and exit of the plateaus. The average of the data in between the entry and the exit is taken as the POI. Protocol of the WP2 of the CCT-WG5 HTFP Research Plan [15] defined a way of POI determination by performing a cubic fit of the experimental data and locating the time when the second derivative is zero. This method was used as our second method, but the second derivative was calculated based on differences of the adjacent data in the corresponding time instead of performing fitting of the data. The time with the second derivative as zero was then obtained and the corresponding signal was identified. Histogram procedure was adopted as the third method. In this procedure, the flattest part of the plateau was used to calculate the average signal which was used to determine the POI. To generate the histogram, a signal step equivalent to temperature step of approximately 50 mK was used. Finally, the standard deviations of data obtained by using these three methods were calculated and analyzed. It is found that the average standard deviation is about 65 mK for Co–C and 45 mK for Pd–C. This is significantly inferior to that of the previous study on shorter cells with average standard deviation of about 20 mK for both cells [13].

In order to compare with the previous results using INRIM cells, the transition temperatures calculated based on the histogram method are adopted as final results where the average standard deviation of the three POI identification methods is considered as the uncertainty of POI definition.

4.2 Determination of Transition Temperatures

The transition temperatures of the two cells are determined by the reference radiation thermometer introduced in Sect. 3 for both furnaces individually and are then averaged between the two furnaces. The calculated ITS-90 temperatures of the POIs of Co–C and Pd–C are given in Table 2. The given values are corrected for emissivity, and SSE

Table 2 ITS-90 temperatures of NMC cells with combined uncertainty

	T_{90} of NMC cell (°C)	T_{90} of INRIM cell (°C) [13]	T_{90} (°C) [16]	T (°C) [17,18]
Co–C	1324.18	1324.03	1324.0	1324.24
	±0.44	±0.29	±0.30	±0.063
Pd–C	1491.61	1491.20	1491.7	1492.04
	±0.31	±0.28	±0.35	±0.13

The figures in the last column are the latest thermodynamic temperature definitions for Co–C [17] and Pd–C [18] listed for benchmarking

Table 3 Uncertainty components

Uncertainty component	Co–C	Pd–C
ITS-90 realization	0.110	0.168
POI definition	0.065	0.045
Plateau repeatability	0.056	0.063
SSE correction	0.029	0.055
Emissivity correction	0.004	0.005
Furnace difference (standard deviation of average)	0.416	0.247
Combined ($k = 1$)	0.44	0.31

effects. The measurement uncertainty components arise from the realization of ITS-90, plateau repeatability, POI definition, emissivity and size-of-source (SSE) corrections, and the differences between the two furnaces are given in Table 3. The combined standard uncertainties with $k = 1$ are estimated to be 0.44 K and 0.31 K for Co–C and Pd–C, respectively. The major uncertainty contribution is the difference between the three-zone furnace and the single-zone furnace which is about 0.59 K and 0.35 K for Co–C and Pd–C, respectively, based on the average of several plateaus for each furnace. This is significantly larger than that obtained in the previous study on smaller and shorter cells which is about 0.35 K and −0.04 K for Co–C and Pd–C, respectively [13]. In that study, the ITS-90 temperatures of the POIs of INRIM cells, given in Table 2 for comparison purposes, were obtained using the same reference radiation thermometer and the same furnaces under the same furnace arrangements. In addition, two working wavelengths, namely 650 nm and 900 nm, were used and the results of the two wavelengths were averaged to obtain a single result for each furnace. This is the only difference with the current study in which only 650 nm is used. As can be seen, the transition temperatures agree within the combined uncertainties for Co–C cells and within the expanded uncertainties for the Pd–C cells. The combined uncertainty for the NMC cell is significantly larger than that of the INRIM cell in the case of Co–C. This is due to the larger difference between the two furnaces as indicated earlier. In the case of the Pd–C cell, the combined standard uncertainties are similar for the two cells despite the slightly larger furnace difference for the NMC cell. This is due to the slightly larger difference of the two working wavelengths in the three-zone furnace for the INRIM cell. The NMC cell transition temperatures are also compared with the

Sadli et al. values [16]. The agreement is within $k = 1$ uncertainty for both Co–C and Pd–C cells, and the uncertainties are also comparable. The latest thermodynamic temperature definitions for Co–C [17] and Pd–C [18] are listed in the same table for benchmarking.

4.3 Quality of the Plateaus

The second analysis of the melting curves is to study the shapes and the durations of the melting curves. To do so, plateaus of the NMC and INRIM cells obtained in the single-zone furnace with very similar furnace settings are compared. Figures 4 and 5 show typical curves for Co–C and Pd–C, respectively, with melts induced by furnace temperatures from (10/5) K below the melting temperature to (10/15) K above the melting temperature. To facilitate the comparison, dimensions and weights of the

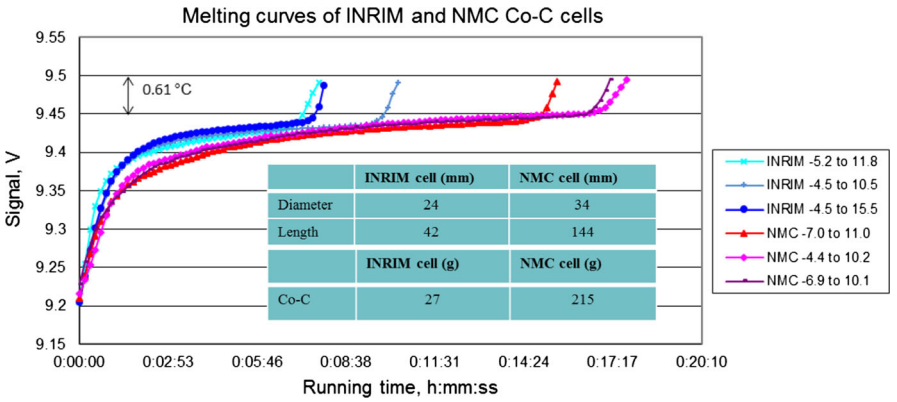

Fig. 4 Melting curves of INRIM and NMC Co–C cells obtained with the single-zone furnace at similar furnace settings together with cell dimensions and weights

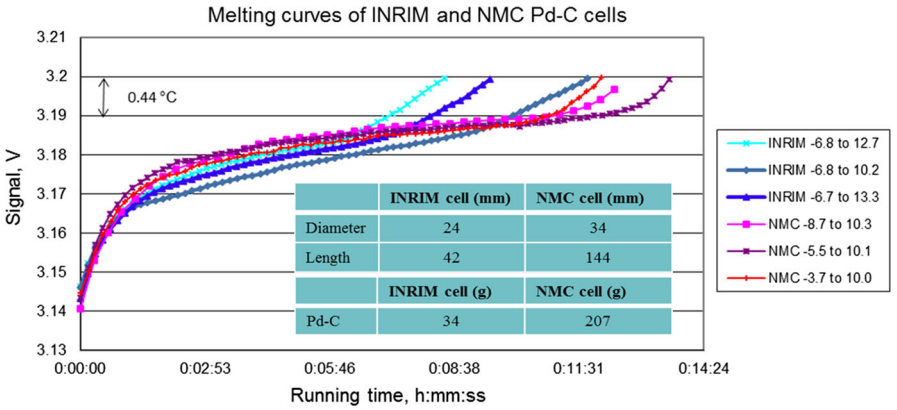

Fig. 5 Melting curves of INRIM and NMC Pd–C cells obtained with the single-zone furnace at similar furnace settings together with cell dimensions and weights

cells are illustrated in the figures as well. For the Co–C cell, the NMC curves are very similar to those of INRIM, but the melting ranges are a little bit wider, which is possibly caused by a larger temperature non uniformity across the NMC cell being much longer than the INRIM cell. For the Pd–C cell, the NMC curves appear to be flatter despite being longer. This is likely due to the inferior quality of the INRIM cell. As a matter of fact, the INRIM cell used for that study has a lower transition temperature as compared with the Sadli et al. T_{90} value [16], which is already lower than the Anhalt et al. T value [18]. For both cells, the NMC curves last longer than the INRIM curves, likely due to the much bigger mass of NMC cells.

Plateaus of the NMC and INRIM cells obtained using the three-zone furnace are compared in the same way as well. Conclusions similar to those of the single-zone furnace are obtained.

4.4 Influence of Furnace

As discussed earlier, the transition temperatures obtained with the three-zone tube furnace are higher than those obtained with the single-zone furnace for both cells. This can be illustrated by typical melting curves obtained with the two furnaces as shown in Figs. 6 and 7. It is worth to note that the two curves in each figure are only typical ones with raw reference thermometer data and are used to show the differences indicatively. The accurate differences are based on average of several plateaus as discussed earlier. Besides the difference in transition temperature, the plateaus obtained with the three-zone furnace are significantly smoother and longer than those obtained with the single-zone furnace for both cells. This is likely due to the higher thermal inertia of the furnace assembly and the slower heating rate of the three-zone furnace. In addition, the more uniformed three-zone tube furnace makes a sharper entrance to the plateau than the single-zone furnace, but the higher thermal inertia and the slower heating rate drag the plateau further and make a more rounded

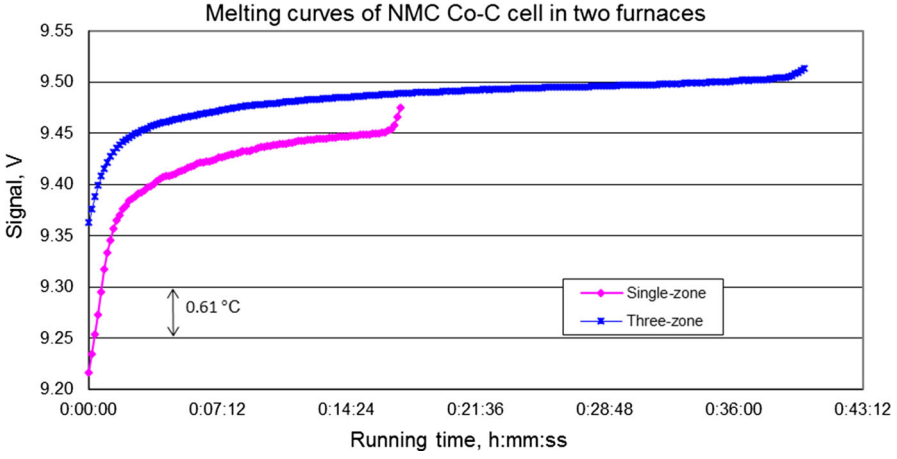

Fig. 6 Typical melting curves of Co–C cell obtained with two furnaces

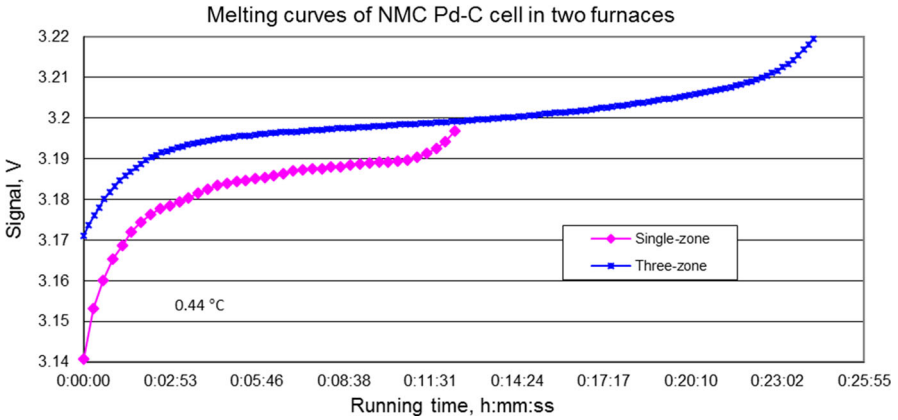

Fig. 7 Typical melting curves of Pd–C cell obtained with two furnaces

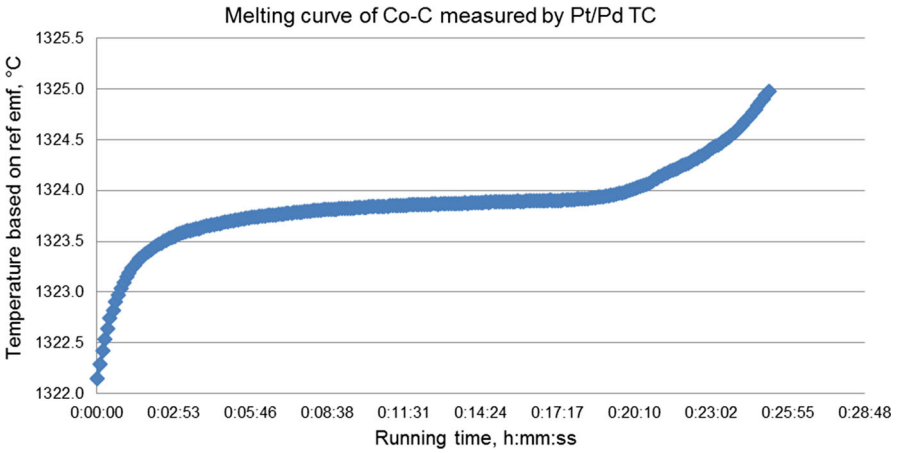

Fig. 8 Melting curve of Co–C cell measured by a Pt/Pd thermocouple

exit of the plateau. As a result, the melting range is about the same overall for the two furnaces. This behavior is not so obvious for the smaller and shorter cells used for the previous study, due to much smaller masses of those cells [13].

5 Measuring with Thermocouple

A preliminary study on thermocouple calibration using the developed Co–C and Pd–C cells was carried out. In this study, the Co–C and Pd–C cells were used to measure a Pt/Pd thermocouple with the single-zone furnace in vertical position but with the same configuration as in horizontal position. The melting plateaus are very similar to those obtained with the reference radiation thermometer as evidenced in Figs. 8 and 9. A more detailed study, such as an investigation into the thermocouple immersion characteristics, measurements with the single-zone furnace, and with the three-zone

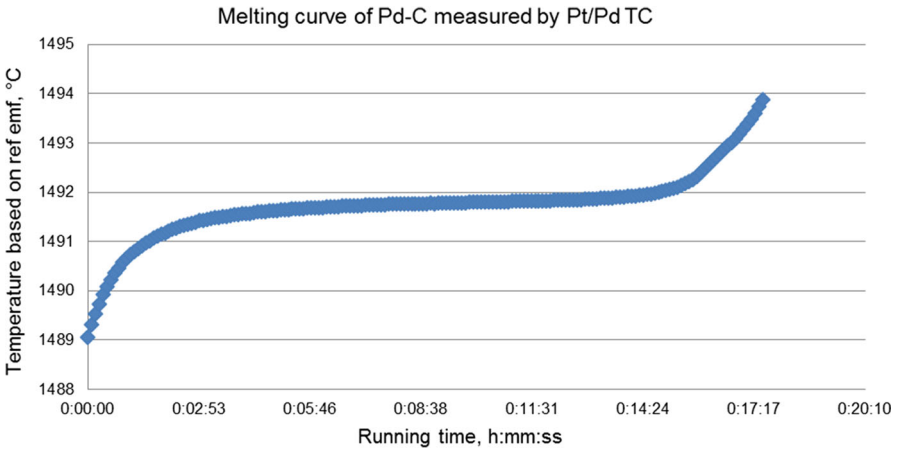

Fig. 9 Melting curve of Pd–C cell measured by a Pt/Pd thermocouple

furnace horizontally, is in the pipeline in order to get a full calibration. In addition, the current Co–C measurement uncertainty is still larger than the existing NMC thermocouple calibration facility, which has a combined uncertainty of 0.26 K at 1300 °C [14], due to the larger difference among the two furnaces. With further study and improvement on the uniformity of the furnaces, a better agreement is expected. The measurement results obtained with the eutectic points and the existing thermocouple calibration facility will then be compared.

6 Conclusions

NMC developed Co–C and Pd–C cells for both radiation thermometer and thermocouple applications. Both cells were evaluated with a reference radiation thermometer. The transition temperatures in terms of ITS-90 were determined to be 1324.18 °C and 1491.61 °C with the corresponding combined standard uncertainties of 0.44 °C and 0.31 °C for Co–C and Pd–C, respectively, taking into account the differences of the two different types of furnaces used. The transition temperatures were compared with those of INRIM small cells obtained in the same furnaces under the same conditions. The agreements were within the combined uncertainties for Co–C cells and within the extended uncertainties for the Pd–C cell. The plateaus obtained with the two furnaces were compared for both NMC cells. Plateaus of both NMC cells were also compared with those of INRIM small cells for each furnace. The comparison results show that the furnace effects on the NMC cells in terms of transition temperature are significantly larger than those of small cells. Nevertheless, the developed NMC cells are sufficient for both radiation thermometer and thermocouple calibrations, although when time and budget permit a small cell might be developed to achieve a better uncertainty for radiation thermometer application. A more detailed investigation in using the cells for thermocouple calibration is planned for the near future.

Acknowledgements The author wishes to thank Y. Yamada, Dr H. Ogura, and Dr F. Girard for their insightful discussions and suggestions offered in the process of this study. Thanks also go to S.H. Ang for his help in literature survey and drawing of the cells and Goh Choon Heng for his assistance in furnace operations and measurements.

References

1. Y. Yamada et al., Radiometric observation of melting and freezing plateaus for a series of metal–carbon eutectic points in the range 1330 °C to 1950 °C. Metrologia **36**, 207 (1999)
2. Y. Yamada et al., High-temperature fixed points in the range 1150 °C to 2500 °C using metal–carbon eutectics. Metrologia **38**, 213 (2001)
3. G. Machin et al., A concerted international project to establish high-temperature fixed points for primary thermometry. Int. J. Thermophys. **28**, 1976–1982 (2007)
4. M. Battuello, F. Girard, M. Florio, Metal–carbon eutectics to extend the use of the fixed-point technique in precision IR thermometry. Int. J. Thermophys. **29**, 926–934 (2008)
5. P. Bloembergen, Y. Yamada, Measurement of thermodynamic temperature above the silver point on the basis of the scheme $n = 2$. Int. J. Thermophys. **32**, 45–67 (2011)
6. F. Edler, A.C. Baratto, A cobalt–carbon eutectic fixed point for the calibration of contact thermometers at temperatures above 1100 °C. Metrologia **42**, 201–207 (2005)
7. H. Ogura, M. Izuchi, M. Arai, Evaluation of cobalt–carbon and palladium–carbon eutectic point cells for thermocouple calibration. Int. J. Thermophys. **29**, 210–221 (2008)
8. J.V. Pearce et al., Evaluation of the Pd–C eutectic fixed point and the Pt/Pd thermocouple. Metrologia **46**, 473–479 (2009)
9. A.D.W. Todd et al., Cobalt–carbon eutectic fixed point for contact thermometry. Int. J. Thermophys. **32**, 453–462 (2011)
10. R.N. Teixeira, A.C. Baratto, A Nickel–carbon eutectic cell for contact and non-contact thermometry. Int. J. Thermophys. **28**, 1993–2001 (2007)
11. F. Edler, J. Hartmann, Simultaneous contact and non-contact measurements of the melting temperature of a Ni–C fixed-point cell. Int. J. Thermophys. **28**, 2002–2008 (2007)
12. J. Bojkovski et al., Design, construction, and evaluation of Ni–C eutectic fixed points. Int. J. Thermophys. **32**, 1800–1810 (2011)
13. M. Battuello, L. Wang, F. Girard, S.H. Ang, Co–C and Pd–C fixed points for the evaluation of facilities and scales realisation at INRIM and NMC, international symposium on temperature and thermal measurement in industry and science—TEMPMEKO 2013, Madeira, Portugal, 14–17 Oct 2013. Int. J. Thermophys. **35**, 535–546 (2014)
14. M. Battuello, F. Girard, L. Wang, INRIM-NMC comparison of Pt/Pd calibration above the Ag point, joint international symposium on temperature, humidity, moisture and thermal measurements in industry and science—TEMPMEKO & ISHM 2010, Portorož, Slovenia, May 31–June 3, 2010. Int. J. Thermophys. **31**, 1444–1455 (2010)
15. Y. Yamada, Protocol CCT-WG 5 HTFP Research Plan, Workpackage 2: Construction of HTFP cells for definitive thermodynamic temperature measurements, Version 3.1 (2010)
16. M. Sadli, et al., Review of metal–carbon eutectic temperatures: proposal for new ITS-90 secondary points. in Proceedings of the TEMPMEKO'04, 9th international symposium on temperature and thermal measurement in industry and science (2005), pp. 341–347
17. E.R. Woolliams et al., Thermodynamic temperature assignment to the point of inflection of the melting curve of high-temperature fixed points. Phil. Trans. R. Soc. A **374**, 20150044 (2016). https://doi.org/10.1098/rsta.2015.0044
18. K. Anhalt et al., Thermodynamic temperature determinations of Co–C, Pd–C, Pt–C and Ru–C eutectic fixed-point cells. Metrologia **43**, S78 (2006)